

Indirect inactivation of tyrosinase in its action on tyrosine

Jose Luis Muñoz-Muñoz¹, Francisco Garcia-Molina¹, Jose Ramon Acosta-Motos¹, Enrique Arribas², Pedro Antonio Garcia-Ruiz³, Jose Tudela¹, Francisco Garcia-Cánovas¹✉ and Jose Neptuno Rodríguez-López¹

¹GENZ: Grupo de Investigación Enzimología, Departamento de Bioquímica y Biología Molecular-A, Facultad de Biología, Universidad de Murcia, Espinardo, Murcia, Spain; ²Departamento de Física Aplicada, Escuela Politécnica Superior de Albacete, Universidad de Castilla la Mancha, Albacete, Spain; ³QCBA: Grupo de Química de Carbohidratos y Biotecnología de Alimentos, Departamento de Química Orgánica, Facultad de Química, Universidad de Murcia, Espinardo, Murcia, Spain

Under aerobic conditions, tyrosinase is inactivated by dopa as a result of suicide inactivation, and, under anaerobic conditions, as a result of irreversible inactivation. However, tyrosine protects the enzyme from being inactivated by dopa under anaerobic conditions. This paper describes how under aerobic conditions the enzyme acting on tyrosine is not directly inactivated but undergoes a process of indirect suicide inactivation provoked by reaction with the o-diphenol originated from the evolution of o-dopaquinone and accumulated in the reaction medium.

Keywords: o-diphenol, monophenol, inactivation, suicide, tyrosinase.

Received: 09 December, 2010; **revised:** 09 November, 2011; **accepted:** 02 December, 2011; **available on-line:** 20 December, 2011

✉ e-mail address: canovasf@um.es

Abbreviations: For clarity and for the sake of brevity, we will use the following notations in the text.

Species and concentrations. $[E]_0$, initial concentration of tyrosinase; E_a , active enzyme; $[E_a]$, instantaneous concentration of E_a ; $[E_m]$, instantaneous concentration of *met*-tyrosinase; $[E_m]_0$, initial concentration of *met*-tyrosinase; $[E_d]$, instantaneous concentration of *deoxy*-tyrosinase; $[E_d]_0$, initial concentration of *deoxy*-tyrosinase; E_d^+ , *deoxy*-tyrosinase after of E_d to E_d^+ transition; $[E_d^+]$, instantaneous concentration of E_d^+ ; $[E_d^+]_0$, initial concentration of E_d^+ ; E_i , inactive enzyme; $[E_i]$, instantaneous concentration of E_i ; D, L- or D-*o*-diphenol (dopa); $[D]_0$, initial concentration of D; $[D]_{ss}$, *o*-diphenol concentration in the steady-state; Q, *o*-quinone product of the enzymatic reaction; $[Q]$, instantaneous concentration of Q; $[Q]_{ss}$, *o*-quinone concentration at $t \rightarrow \infty$; $[NADH]_0$, initial concentration of NADH; $[NADH]$, instantaneous concentration of NADH; $[NADH]_{ss}$, NADH concentration at $t \rightarrow \infty$; $[NADH]_{con}$, NADH consumed at the end of the reaction, $t \rightarrow \infty$, i.e. $[NADH]_{ss} = [NADH]_0 - [NADH]_{con}$; M, L- or D-*o*-monophenol (tyrosine); $[M]_0$, initial concentration of monophenol; $[M]_{ss}$, monophenol concentration in the steady-state; C, relationship between *o*-diphenol and monophenol concentrations in the steady-state, $C = [D]_{ss} / [M]_{ss}$; DC, dopachrome; $[DC]$, instantaneous concentration of DC; $[DC]_{ss}$, dopachrome concentration at $t \rightarrow \infty$; $[O_2]_0$, initial concentration of oxygen; $[O_2]$, instantaneous concentration of oxygen; $[O_2]_t$, oxygen concentration at $t \rightarrow \infty$; $[O_2]_{con}$, oxygen consumed at $t \rightarrow \infty$, i.e. $[O_2]_{ss} = [O_2]_0 - [O_2]_{con}$; R, reductant; $[R]_0$, initial concentration of R; $[R]$, instantaneous concentration of R; $[R]_t$, $[R]$ concentration at $t \rightarrow \infty$; $[R]_{ss}$, $[R]$ concentration at $t \rightarrow \infty$, i.e. $[R]_{ss} = [R]_0 - [R]_{con}$.

Kinetic parameters. $V_0^{D(Q)}$, initial rate of tyrosinase acting on D, measuring Q; $V_0^{D(DC)}$, initial rate of tyrosinase acting on D, measuring DC; $V_0^{D(DC)} = 0.5 V_0^{D(Q)}$; $V_0^{D(O_2)}$, initial rate of tyrosinase acting on D, measuring O_2 ; $V_0^{D(O_2)} = V_0^{D(DC)}$; $\lambda_{E_a}^M$, apparent suicide inactivation constant of tyrosinase in the presence of monophenol; $\lambda_{E_{ox}}^M$, maximum value of $\lambda_{E_{ox}}^M$ for saturating substrate; $\lambda_{E_d}^{D(L \text{ or } D)(M)}$, apparent constant of irreversible inhibition of E_d by L- or D-dopa, in the presence of the monophenol L- or D-tyrosine; $\lambda_{E_d}^{D(L \text{ or } D)(M)}$, apparent constant of irreversible inhibition of E_d^+ by L- or D-dopa, in the presence of the monophenol L- or D-tyrosine; $k_{D(L \text{ or } D)(M)}$, maximum value of $\lambda_{E_d}^{D(L \text{ or } D)(M)}$ for saturating substrate; $k_{D(L \text{ or } D)(M)}^*$, maximum value of $\lambda_{E_d}^{D(L \text{ or } D)(M)}$ for saturating substrate; r_D^{DC} , partition ratio for the diphenolase activity measuring DC; $r_D^{O_2}$, partition ratio for the diphenolase activity measuring O_2 ; $r_D^{NADH} = r_D^{DC} = r_D^{O_2}$ with $[NADH]_{ss} = 2[DC]_{ss} = [Q]_{ss}$ and $[DC]_{ss} = [O_2]_{con}$; $r_{Mr}^{O_2}$, number of total turnovers (in both cycles, hydroxylase and oxidase) made by one molecule of enzyme acting on L-tyrosine before its suicide inactivation, measuring oxygen consumed; $r_{M(O)}^{O_2}$, number of turnovers in the oxidase cycle made by one molecule of enzyme acting on L-tyrosine before its suicide inactivation, measuring oxygen consumed; $r_{M(H)}^{O_2}$, number of turnovers in the hydroxylase cycle made by one molecule of enzyme acting on L-tyrosine before its suicide inactivation, measuring oxygen consumed; r_M^{DC} , number of total turnovers (in both cycles) made by one molecule of enzyme acting on L-tyrosine before its suicide inactivation, measuring dopachrome formed; $r_{M(O)}^{DC}$, number of turnovers in the oxidase cycle made by one molecule of enzyme acting on L-tyrosine before its suicide inactivation, measuring dopachrome formed; $r_{M(H)}^{DC}$, number of turnovers in the hydroxylase cycle made by one molecule of enzyme acting on L-tyrosine before its suicide inactivation, measuring the dopachrome formed; $K_m^{D(L \text{ or } D)}$, Michaelis constant of tyrosinase for L- or D-tyrosine; $K_{E_d}^{D(L \text{ or } D)}$, catalytic constant of the monophenolase activity for L- or D-tyrosine; $K_d^{D(L \text{ or } D)(M)}$, dissociation constant of the complex E_d^+D , where D is L-dopa, in the presence of the monophenol L- or D-tyrosine; $K_{E_d}^{D(L \text{ or } D)}$, dissociation constant of the complex E_d^+M , where M is L- or D-tyrosine; $K_d^{D(L \text{ or } D)(M)}$, dissociation constant of the complex E_dD , where D is L-dopa in the presence of the monophenol L- or D-tyrosine; $K_{E_d}^{D(L \text{ or } D)}$, dissociation constant of the complex E_dM , where M is L- or D-tyrosine.

Waley, 1980; 1985; Garcia-Canovas *et al.*, 1987; Tudela *et al.*, 1987). These studies have enabled the critical parameters of the suicide inactivation of the enzyme to be determined: k_{cat} , the catalytic constant; K_m , the Michaelis constant; r , number of turnovers made by one mole of enzyme before its suicide inactivation and λ_{max} (maximum apparent inactivation constant).

The progress made in the study of the tyrosinase structure, with the crystallization of the enzyme from *Streptomyces castaneoglobisporus* (Matoba *et al.*, 2006), *Bacillus megaterium* (Sendovski *et al.*, 2010; 2011), and *Agaricus bisporus* (Ismaya *et al.*, 2011) has provided better insight into the underlying mechanisms of the suicide inactivation of tyrosinase (Muñoz-Muñoz *et al.*, 2008; 2010a; 2010b; Chazarra *et al.*, 1997; Chang, 2007; 2009; 2010; Tai *et al.*, 2009; Land *et al.*, 2007; 2008; Ramsden *et al.*, 2009; Ramsden & Riley, 2010a; 2010b).

The suicide inactivation of tyrosinase acting on L-tyrosine (as an example of monophenols) is difficult to study because the enzyme shows a lag period (Rodríguez-Lopez *et al.*, 1992a; Molina *et al.*, 2007). Furthermore, the enzyme transforms L-tyrosine into L-dopa and this, in turn, into *o*-dopaquinone, which evolves towards dopachrome and L-dopa (Cabanés *et al.*, 1987). This series of chemical reactions leads to the accumulation of L-dopa in the medium and, in this way, tyrosinase reaches the steady state (Rodríguez-Lopez *et al.*, 1992a and Ros *et al.*, 1994). In this situation, tyrosinase carries out two turnovers in the monophenolase pathway but only one in the diphenolase pathway (Rodríguez-Lopez *et al.*, 1992a).

Although the action mechanism of tyrosinase on L-tyrosine is complex (Sanchez-Ferrer *et al.*, 1995), some important aspects are known about it; for example, for the oxidation to occur there must be an electrophilic attack on the benzene ring (Karlín *et al.*, 1998; Itoh & Fukuzumi, 2007) and the substrate must be deprotonated before it can be oxidised (Casella *et al.*, 1996; Monzani *et al.*, 1998).

Two models, which share certain aspects and diverge considerably in others (Schemes I–III and IV), have been proposed to explain the suicide inactivation of tyrosinase in its action on *o*-diphenolic substrates (Land *et al.*, 2007; Muñoz-Muñoz *et al.*, 2008). In both cases, it is suggested that one of the copper atoms at the active centre is reduced to Cu^0 and is released, thus inactivating the enzyme (Dietler & Lerch, 1982). Other authors (Land *et al.*, 2007) suggest (Scheme IV) that the enzyme hydroxylates the *o*-diphenols because it considers them as another form of monophenol. According to this model, a compound like pyrogallol (1,2,3-trihydroxybenzene) would not lead to suicide inactivation of the enzyme. In a previous work, our group showed that all *o*-diphenols and triphenols are suicide substrates of tyrosinase, the most potent being pyrogallol (Muñoz-Muñoz *et al.*, 2008). The mechanism proposed in Schemes I–III covers the possibility of suicide inactivation during the oxidation of *o*-diphenols and triphenols like gallic acid or pyrogallol since it is the way in which one proton of the substrate is transferred to the active centre of the enzyme which triggers its suicide inactivation.

In the structural mechanism described in Scheme ISM (Supplementary Material), and in its kinetic form (Scheme I), we propose that the enzyme does not suffer inactivation in its hydroxylase activity, but that this inactivation occurs in its action on the diphenol accumulated in the reaction medium (Munoz-Munoz *et al.*, 2008; 2010a; 2010b). Scheme ISM proposes the transfer of a

proton from monophenols or diphenols to the peroxide of the oxy-tyrosinase form of the enzyme. Such a transfer step was previously proposed by Tyeklar and Karlín (1989) working with copper complexes and by Miller and Klinman (1985) to explain the action of dopamine β -hydroxylase. More recently, the transfer of a proton from the monophenol to the peroxide, which acts as a catalytic base, has been proposed (Matoba *et al.*, 2006). The transfer of this critical proton to the oxy-tyrosinase form has been considered in studies on the isotopic effect as the slow step of the process both in *o*-diphenols and monophenols (Peñalver *et al.*, 2003; Fenoll *et al.*, 2004). There is controversy as to whether the initial step of the substrate oxidation occurs on the CuA (Decker *et al.*, 2006) or CuB (Matoba *et al.*, 2006). We suggest that in the case of *o*-diphenols it occurs in the second transfer of a proton to the hydroperoxide, when it forms H_2O_2 , reducing the copper to Cu^0 and inactivating the enzyme (see Scheme ISM).

Taking into consideration the mechanisms proposed to explain this suicide inactivation (Land *et al.*, 2007; Munoz-Munoz *et al.*, 2008), the aim of the present study was to establish the criteria necessary to be able to discriminate between the two models (Scheme III, inactivation through the diphenolase activity and Scheme IV, inactivation through the monophenolase activity).

MATERIAL AND METHODS

Materials. Mushroom tyrosinase or polyphenol oxidase (Tyr; *o*-diphenol:O₂ oxidoreductase, EC 1.14.18.1) (8300 units/mg) and β -NADH were supplied by Sigma (Madrid, Spain). The enzyme was purified as previously described in (Rodríguez-Lopez *et al.*, 2000). Protein concentration was determined by the Lowry method (Lowry *et al.*, 1951). The substrates used, L-dopa, D-dopa, L-tyrosine and D-tyrosine were purchased from Sigma. All other chemicals were of analytical grade. Stock solutions of the diphenolic substrates were prepared in 0.15 mM phosphoric acid to prevent autooxidation. Milli-Q system (Millipore Corp.) ultrapure water was used throughout the experiments.

Spectrophotometric assays. Diphenolase activity. These assays were carried out with a Perkin-Elmer Lambda-35 spectrophotometer, interfaced to a PC-computer, where the kinetic data were recorded, stored and later analyzed. The product of the enzyme reaction, *o*-dopaquinone, is unstable and evolves towards dopachrome, which is not stable at long assay times (García-Carmona *et al.*, 1982; García-Canovas *et al.*, 1982). For this reason, the reaction was followed by measuring the disappearance of NADH at 340 nm, with $\epsilon=6230 \text{ M}^{-1}\cdot\text{cm}^{-1}$, which reduces *o*-dopaquinone to L-dopa (García-Molina *et al.*, 2007). The inactivation kinetics was studied in 30 mM sodium phosphate buffer (pH 6.0), since *o*-dopaquinone evolves rapidly to dopachrome at pH 7.0, while at lower pH the reaction slows down and *o*-dopaquinone is reduced by NADH (García-Canovas *et al.*, 1982).

Monophenolase activity. These assays were carried out with the same apparatus as used in the diphenolase activity assays. The reaction was followed by measuring dopachrome accumulation in the reaction medium at $\lambda=475 \text{ nm}$ ($\epsilon=3600 \text{ M}^{-1}\cdot\text{cm}^{-1}$) (García-Molina *et al.*, 2007). The inactivation kinetics was studied in 30 mM sodium phosphate buffer (pH 7.0). A given quantity of *o*-diphenol was always added at $t=0$, $C=[D]_{\text{ss}}/[M]_{\text{ss}}=0.046$,

so that the steady-state was reached immediately (Ros *et al.*, 1994).

Oxymetric assays. Measurements of dissolved oxygen concentration were made with a Hansatech (Kings Lynn, Cambs, UK) oxygraph unit controlled by a PC. The oxygraph used a Clark-type silver/platinum electrode with a 12.5 mm Teflon membrane. The sample was continuously stirred during experiments and its temperature was maintained at 25 °C. The zero oxygen level for calibration and experiments was obtained by bubbling oxygen-free nitrogen through the sample for 10 min (Rodríguez-Lopez *et al.*, 1992b). The substrates L-tyrosine and D-tyrosine were studied by means of this method, adding (at $t=0$) the quantity of *o*-diphenol necessary for the steady-state to be attained immediately (Ros *et al.*, 1994).

Kinetic data analysis of monophenolase activity. The experimental recordings of oxygen consumption in the action of tyrosinase on monophenol fit Eqn. (1):

$$[O_2] = [O_2]_f + [O_2]_{\infty} e^{-\lambda_{E_{ox}}^M t} \quad (1)$$

whose parameters can be obtained by non-linear regression (Jandel, 2006). Thus, the experimental recordings obtained fit Eqn. (1), from which the corresponding inactivation parameters, $[O_2]_{\infty}$ and $\lambda_{E_{ox}}^M$, can be determined.

Simulation assays. The simulation reveals the kinetic behavior of the concentrations of the ligand and enzymatic species involved in the reaction mechanism here proposed for tyrosinase. The respective systems of differential equations have been solved numerically for particular sets of values of the rate constants and of initial concentrations of the reaction mechanism species. The numerical integration is based on the Runge–Kuta–Fehlberg algorithm, implemented on a PC-compatible computer program (WES) (García-Sevilla *et al.*, 2000).

Simulated data of time based assays for the accumulation of dopachrome, or for the disappearance of the coupled reductant R, were fitted to Eqns. (2) and (3), respectively (see Supplementary material):

$$[DC] = [DC]_{\infty} (1 - e^{-\lambda_{E_{ox}}^{D \text{ or } M} t}) \quad (2)$$

$$[R] = [R]_f + [R]_{\infty} e^{-\lambda_{E_{ox}}^{D \text{ or } M} t} \quad (3)$$

Generation of E_{ox} and E_d . To kinetically characterize the inactivation of the E_d form of tyrosinase, this enzymatic form was generated from the native enzyme by adding micromolar concentrations (2 μ M) of H_2O_2 , so that the E_m form passed to E_{ox} . Then, nitrogen was bubbled through the solution transforming all the E_{ox} to E_d ($E_{ox} \xrightarrow{N_2} E_d + O_2$) (Jolley *et al.*, 1974; Beltramini & Lerch, 1982; Jackman *et al.*, 1992; Muñoz-Munoz *et al.*, 2009).

Generation of E_d^* . To kinetically characterize the inactivation of the E_d^* form of tyrosinase, this enzymatic form was generated from the E_d^* form and, maintaining anaerobic conditions, E_d^* was allowed to evolve slowly towards the enzymatic form that we denominate E_d^* (Muñoz-Munoz *et al.*, 2010c).

Generation of E_m . The inactivation of E_m was characterized by first generating it from the native enzyme in two ways: (a) Adding 2 μ M catalase, so that $E_{ox} \xrightarrow{C} E_m + H_2O_2$; the catalase acts on the H_2O_2 displacing the above equilibrium $2H_2O_2 + \text{catalase} \rightarrow O_2 + 2H_2O$, so that all E_{ox} is transformed into E_m by the end of the reaction. (b) Adding 2 μ M of H_2O_2 , so that the entire enzyme passes to E_{ox} and then adding 2 μ M catalase

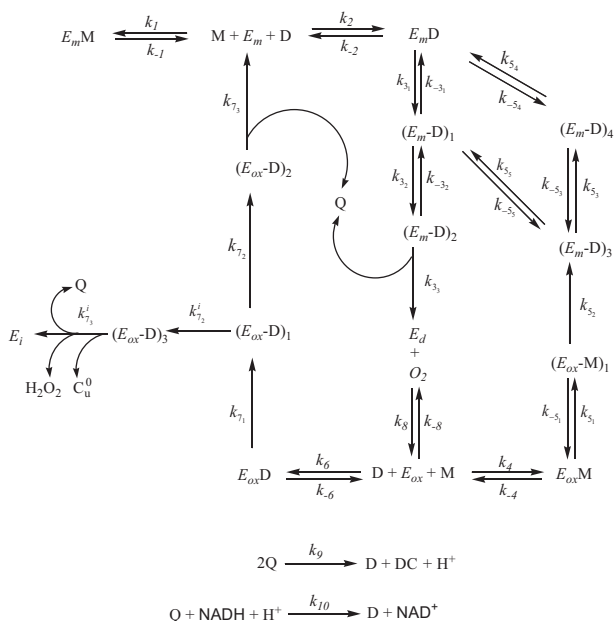
(Muñoz-Munoz *et al.*, 2009). E_m was generated to study its possible inactivation by monophenols.

Evaluation of enzymatic species E_m , E_d , and E_{ox} in an enzymatic preparation of tyrosinase. It is known that an enzymatic preparation of tyrosinase from any source is found in three forms, E_m , E_d and E_{ox} (Jackman *et al.*, 1992). Several authors have proposed spectrophotometric methods for evaluating these forms (Jolley *et al.*, 1974; Deinum *et al.*, 1976; Jackman *et al.*, 1992). Here, we propose a kinetic method based on the fact that their inactivation by 2-mercaptoethanol (Aasa *et al.*, 1978) occurs over a wide time range: inactivation constants of 0.014 s⁻¹, 4 × 10⁻⁵ s⁻¹ and 1 × 10⁻⁵ s⁻¹ for E_{ox} , E_m and E_d , respectively. Under aerobic conditions at oxygen concentrations of 0.26 mM, practically the only forms existing are E_{ox} and E_{om} (Rodríguez-Lopez *et al.*, 2000). Note that the difference between $k_{E_{ox}}^m$ and $k_{E_m}^m$ is three orders of magnitude, a difference that can be used to evaluate these enzymatic forms. The experimental method used was described in (Muñoz-Munoz *et al.*, 2009).

¹³C-NMR assays. ¹³C-NMR spectra of several substrates were obtained at pH=6.0 in a Varian Unity spectrometer at 300 MHz, using ²H₂O as solvent for the substrates. Chemical displacement (δ) values were measured relative to those for tetramethylsilane ($\delta=0$). The maximum line breadth accepted in the ¹³C-NMR spectra was 0.06 Hz. Therefore, the maximum accepted error for each peak of the spectrum was ± 0.03 p.p.m.

RESULTS AND DISCUSSION

In this work, we study the reaction of the different enzymatic forms that exist in the turnover of tyrosinase with L- and D-tyrosine, that is, the form *oxy*-tyrosinase, under aerobic conditions, and the forms *mel*-tyrosinase and *deoxy*-tyrosinase, under anaerobic conditions

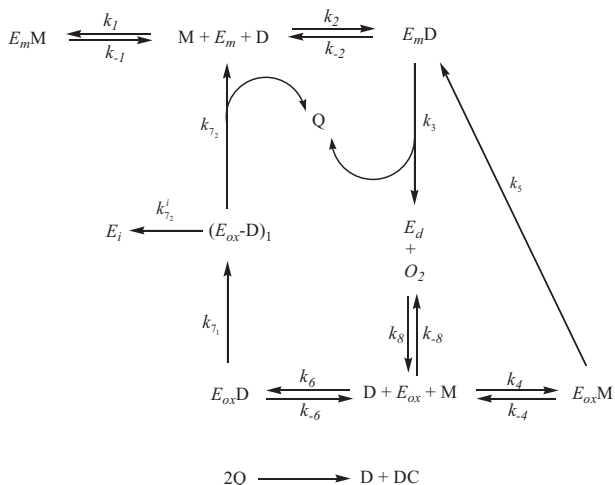


Scheme 1. Kinetic mechanism proposed to explain the monophenolase together with diphenolase and suicide inactivation pathways of tyrosinase action on tyrosine enantiomers (see Scheme ISM for further details).

(Scheme I in the kinetic form and Scheme ISM in the structural form) (Sanchez-Ferrer *et al.*, 1995).

Inactivation of tyrosinase in its action on monophenols under aerobic conditions: suicide inactivation

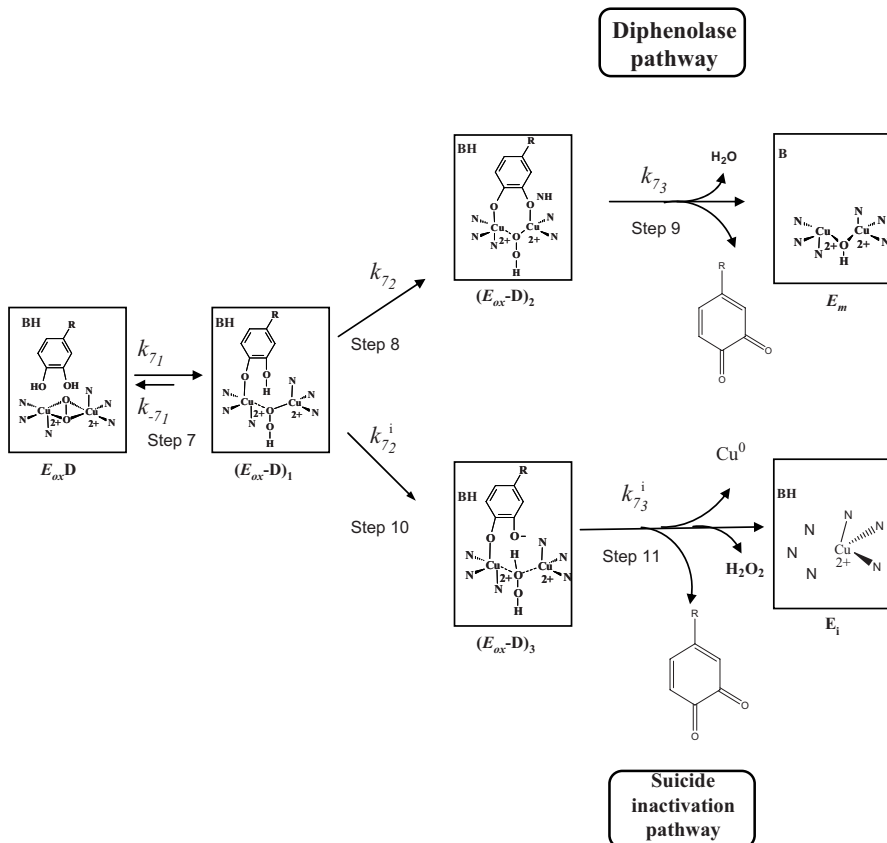
As mentioned above, the model we proposed to explain the suicide inactivation of tyrosinase involves the enzymatic form *oxy*-tyrosinase reacting with an *o*-diphenol in the diphenolase activity (Scheme I and in its simplified form Scheme II) and is based on the structural mechanism proposed in Scheme ISM. It can be outlined as follows:



Scheme II. Simplified kinetic mechanism to explain the monophenolase and diphenolase activities of tyrosinase and the suicide inactivation process.

The kinetic mechanisms described in Schemes I and II and in the structural mechanisms of Scheme ISM suggest that the enzyme is not inactivated in the hydroxylase cycle. For the hydroxylase reaction to take place, the monophenol must transfer a proton to the peroxide, which represents the slow step of the process (Peñalver *et al.*, 2003; Fenoll *et al.*, 2004). The formation of a hydroperoxide has been proposed in copper complexes (Tyeklar & Karlin, 1989), for the hydroxylation of dopamine β -hydroxylase (Miller & Klinman, 1985) and, more recently, in the action of tyrosinase of *Streptomyces castaneoglobisporus* on monophenols (Matoba *et al.*, 2006). Subsequently the electrophilic attack of the oxygen of the peroxide group of the *oxy*-tyrosinase form takes place in a *meta*-position of the benzene ring of the L-tyrosine (Karlin *et al.*, 1998; Itoh & Fukuzumi, 2007). However, in the diphenolase cycle (Schemes I and II), although the first step is also the transfer of a proton from the hydroxyl group on C-4 to the peroxide in the *oxy*-tyrosinase form (Peñalver *et al.*, 2003; Fenoll *et al.*, 2004), the following step (see Matoba *et al.*, 2006) is another transfer of a proton from the hydroxyl group on C-3 to the nitrogen atom of the histidine bound axially to the CuA (catalysis) or to the peroxide group, which acts as a base (inactivation) (Scheme III). Note that this step does not exist in the hydroxylase cycle. However, a kinetic study of the suicide inactivation process with monophenol cannot be carried out experimentally in a rigorous and systematic manner, as it has for *o*-diphenols (Munoz-Munoz *et al.*, 2008; 2010a), for the following reasons:

i) The instability of dopachrome. The dopachrome resulting from the rapid evolution of *o*-dopaquinone, is unstable, and evolves towards indoles (Riley, 1997) (data not shown), which make it impossible to follow the suicide inactivation kinetics of tyrosinase spectrophotomet-



Scheme III. Proposed model to explain the suicide inactivation of tyrosinase during its diphenolase activity when it acts on *o*-diphenols (see Scheme ISM for further details).

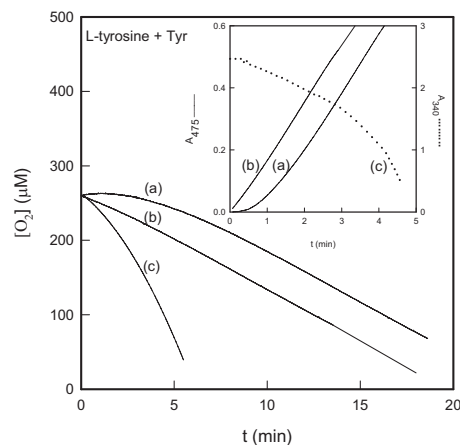


Figure 1. Monophenolase activity of tyrosinase.

Recordings of oxygen consumed in the monophenolase activity of tyrosinase. The experimental conditions were: 30 mM sodium phosphate buffer (pH 6.0), 25°C, $[O_2]_0=0.26$ mM, $[L\text{-tyrosine}]_0=1$ mM, $[Tyr]_0=0.15$ mM, curve (a) $[D]_0=0$; curve (b) $[D]_0=46$ μ M and curve (c), $[D]_0=46$ μ M and $[NADH]_0=0.2$ mM. **Inset.** Recordings of dopachrome accumulation at 475 nm, curves (a) ($[D]_0=0$) and (b) ($[D]_0=46$ μ M), and of disappearance of NADH at 340 nm, curve (c), in the same experiment conditions as described in Fig. 1.

rically by measuring dopachrome. In the case of diphenolase activity, the *o*-quinone can be prevented from evolving by adding NADH to the medium to reduce the *o*-dopaquinone to L-dopa. However, when the enzyme acts on monophenols, the addition of NADH to the reaction medium leads to the continuous accumulation of *o*-diphenol in the medium and the system does not reach the initial steady-state from which the transition phase of the suicide inactivation would occur, Fig. 1, curve (c), and Fig. 1 Inset, curve (c). Note the difference from the kinetics depicted in Fig. 1, curves (a) and (b) and Fig. 1 Inset, curves (a) and (b), which were made in the absence of NADH.

ii) The concentration of monophenol cannot be maintained constant by the presence of the reductant (NADH). The reduction of the *o*-dopaquinone by NADH generates L-dopa, which constantly increases in the medium until the enzyme is inactivated. However, the concentration of monophenol decreases. Note that in the case of monophenolase activity, oxymetric and spectrophotometric short time measurements show that the velocity increases with time in the presence of reductant (parabolic behavior), Fig. 1, curve (c) and Fig. 1 Inset, curve (c), due to the accumulation of *o*-diphenol. Tyrosinase acts better (higher catalytic constant) with *o*-diphenols than with monophenols (Rodríguez-Lopez *et al.*, 1992a).

iii) The inactivation kinetics of tyrosinase acting on monophenols is slower than when it acts on *o*-diphenols. In the case of diphenolase activity (Schemes I and II with $[M]_0=0$), all the enzyme participates in the catalytic cycle, which leads to suicide inactivation at long time-values. However, in the monophenolase activity (Schemes I and II), as was previously demonstrated (Rodríguez-Lopez *et al.*, 1992a), the enzyme in the steady-state makes two turnovers in the hydroxylase cycle for every one in the oxidase cycle. Therefore, in agreement with our hypothesis, the hydroxylase activity does not inactivate the enzyme, but protects it from suicide inactivation. Moreover, much of the *met*-tyrosinase form is reversibly bound to the monophenol as *met*-tyrosinase/monophenol, which further slows the inactivation kinet-

ics. All the above features (dopachrome instability, substrate variation and slowness of the process) means that the reaction cannot be followed by measuring the dopachrome at long times and that NADH cannot be added (Fig. 2, Inset B).

Taking into account all the experimental difficulties described, the only possibility to study the inactivation kinetics experimentally from the monophenolase activity is to measure the consumption of oxygen at high monophenol concentrations (Fig. 2). From these measurements of monophenolase activity and of diphenolase activity, a quantitative relation can be established between the experimentally measurable magnitudes, which give weight to our hypothesis that the enzyme is not inactivated in the hydroxylase cycle. The explanation for this is that the enzyme acting on the *o*-diphenol directly or on the *o*-diphenol accumulated in the steady-state when acting on monophenol, must undergo the same number of turnovers before inactivation. Below, we provide more details as a function of the parameters that can be measured experimentally: $[NADH]_{\infty}$, diphenolase activity and $[O_2]_{\infty}$, monophenolase activity.

If the diphenolase activity is followed spectrophotometrically by measuring the consumption of NADH, the number of turnovers that a molecule of enzyme must make before its suicide inactivation r_D^{NADH} (2 NADH molecules are consumed in each turnover) will be:

$$r_D^{NADH} = \frac{[NADH]_{\infty}/2}{[E]_0} \quad (4)$$

Since, according to our model, the enzyme acting on monophenols is only inactivated through its action on the *o*-diphenol accumulated in the steady-state, one of the difficulties involves the calculation of the number of turnovers made by the enzyme in the diphenolase cycle from the measurements of the monophenolase activity (oxygen consumption). This was done by taking into account: *i*) the stoichiometric relation is $3O_2:2DC$, i.e., 3 molecules of oxygen generate 2 molecules of dopachrome, in the monophenolase activity, *ii*) in the diphenolase cycle only one molecule of DC is formed, consuming one molecule of oxygen, and *iii*) in the hydroxylase cycle two molecules of oxygen are consumed to form one molecule of DC (Rodríguez-Lopez *et al.*, 1992a). The total number of turnovers made by one molecule of enzyme in the monophenolase activity before it is inactivated is:

$$r_M^{O_2} = \frac{[O_2]_{\infty}}{[E]_0} \quad (5)$$

These turnovers would be of two types, the first for the hydroxylase cycle ($r_{M(H)}^{O_2}$, non-inactivating) and the second for the oxidase cycle ($r_{M(O)}^{O_2}$, capable of provoking suicide inactivation) and, in turn, $r_{M(H)}^{O_2} = 2r_{M(O)}^{O_2}$ (Rodríguez-Lopez *et al.*, 1992a).

The formation of one molecule of DC in the oxidase cycle consumes one molecule of oxygen, and in the hydroxylase cycle two molecules of oxygen, so that:

$$r_M^{O_2} = r_{M(H)}^{O_2} + r_{M(O)}^{O_2} = \frac{2}{3} \frac{[O_2]_{\infty}}{[E]_0} + \frac{1}{3} \frac{[O_2]_{\infty}}{[E]_0} = \frac{[O_2]_{\infty}}{[E]_0} \quad (6)$$

To demonstrate that the suicide inactivation of tyrosinase acting on monophenols is indirect, and depending on the *o*-diphenol accumulated in the medium, the ratio of Eqn. (7) should be fulfilled. This equation shows the ratio between the number of turnovers of the enzyme acting on the *o*-diphenol (r_D^{NADH}) and the number

of turnovers of the enzyme acting on the *o*-diphenol accumulated by tyrosinase acting on monophenols and due to the *o*-quinone evolution ($r_{M(O)}^{O_2}$). Expressed as a function of the experimentally measurable parameters, $[NADH]_{\infty}$ and $[O_2]_{\infty}$:

$$\frac{r_D^{NADH}}{r_{M(O)}^{O_2}} = \frac{\frac{[NADH]_{\infty}/2}{[E]_0}}{\frac{[O_2]_{\infty}/3}{[E]_0}} = 1 \quad (7)$$

To check our model (Schemes I–III), two approaches were designed: numerical integration and experimental approach.

Numerical integration of the mechanisms proposed. The numerical integration of the mechanisms proposed in Scheme I in the presence and absence of monophenol ($[M]_0 = 0$) should confirm the predictions indicated in Eqn. (7). If the product of the evolution of *o*-dopaquinone (dopachrome) is considered stable in the numerical integration, the parameters r_D^{DC} should fulfil the following relations:

$$r_D^{DC} = \frac{[DC]_{\infty}^{DC}}{[E]_0} \quad (8)$$

and

$$r_{M(O)}^{DC} = \frac{[DC]_{\infty}^{M/2}}{[E]_0} \quad (9)$$

The ratio between the r_D^{DC} and $r_{M(O)}^{DC}$ should be 1, according to:

$$\frac{r_D^{DC}}{r_{M(O)}^{DC}} = \frac{\frac{[DC]_{\infty}^{DC}}{[E]_0}}{\frac{[DC]_{\infty}^{M/2}}{[E]_0}} = 1 \quad (10)$$

Therefore, the results for the time course of DC formation in the diphenolase and monophenolase activities (oxidase cycle) should fulfil Eqn. (10).

a) Diphenolase activity

i) Absence of reductant. Simulation of the mechanism proposed in Scheme I with $[M]_0=0$, and the analytical solution of the suicide inactivation process according to Scheme II, which is a simplified mechanism of Scheme I, are presented in Supplementary Material.

Variation of enzyme concentration. Figure 1SM depicts the effect of variations in enzyme concentration. The values of $\lambda_{E_{ox}}^D$ and $[DC]_{\infty}^D$ fulfil Eqns. (11) and (12) (Fig. 1SM Inset).

$$[DC]_{\infty}^D = r_D^{DC} [E]_0 \quad (11)$$

with

$$\lambda_{E_{ox}}^D = \frac{\lambda_{E_{ox}(max)}^D [D]_0}{K_m^D + [D]_0} \quad (12)$$

$$r_D^{DC} = \frac{k_2}{k_2^i} \quad (13)$$

$$\lambda_{E_{ox}(max)}^D = \frac{k_{cat}^D}{r_D^{DC}} \quad (14)$$

Variation of substrate concentration. Figure 2SM depicts the variation in substrate concentration and the

Fig. 2SM Inset represents the apparent inactivation constant ($\lambda_{E_{ox}}^D$) vs. $[D]_0$, Eqn. (12).

ii) Presence of reductant. The suicide inactivation of tyrosinase acting on *o*-diphenols in the presence of reductant is simulated in Fig. 3SM. Note that the values of the apparent inactivation constant are equal to those obtained in the absence of reductant. The values of the reductant consumed at the end of the reaction, $[R]_{\infty}$, and the product formed in its absence, $[DC]_{\infty}$, have a ratio of 2 (Fig. 3SM), since the reductant is consumed with a stoichiometry of 1NADH:1Q, i.e. 1 NADH molecule consumes 1 *o*-quinone molecule, while, in its absence, the dopachrome is formed with a stoichiometry of 1DC:2Q, i.e., 1 dopachrome molecule is generated from 2 *o*-quinone molecules. Therefore, the suicide inactivation kinetics of tyrosinase in its diphenolase activity should be studied in the presence of reductant. This is not the situation with the monophenolase activity of tyrosinase, as we shall see below.

b) Monophenolase activity

i) Absence of reductant. The mechanism proposed in Scheme I was simulated by accepting that, at $t=0$, the *o*-diphenol concentration is such that $[D]_{ss}/[M]_{ss}=C$ (Ros *et al.*, 1994), thus avoiding a lag period (see Supplementary Material). The analytical solution of the suicide inactivation process is also described in the Supplementary Material according to Scheme II.

Varying enzyme concentration. Variations in enzyme concentration are shown in Fig. 4SM and Fig. 4SM Inset. The results agree with the kinetic analysis, Eqns. (15–16), and indicate that if experimental measurement were possible, similar results to those for diphenolase activity would be obtained.

According to Eqns. (8–10), the expressions for monophenolase activity are:

$$[DC]_{\infty}^{DC} = 2r_D^{DC} [E]_0 \quad (15)$$

$$\lambda_{E_{ox}}^M = \frac{\lambda_{E_{ox}(max)}^M [M]_0}{K_m^M + [M]_0} \quad (16)$$

$$\lambda_{E_{ox}(max)}^M = \frac{k_{cat}^M}{r_D^{DC}} = \frac{k_{cat}^M}{r_{M(O)}^{DC}} \quad (17)$$

The experimental data of K_m^D and K_m^M (0.5 mM for L-dopa and 0.27 mM for L-tyrosine, respectively) are in the same range, and so the velocity of the process will depend, according to Eqn. (12) and Eqn. (16), on the value of the apparent inactivation constant. According to Eqn. (14) and Eqn. (17), the maximum apparent inactivation constant is related with the catalytic constant and, since $k_{cat}^D > k_{cat}^M$ (110 s^{-1} for L-dopa and 8 s^{-1} for L-tyrosine, respectively), $\lambda_{E_{ox}}^D > \lambda_{E_{ox}}^M$ for the same concentration of the substrate.

Varying the substrate concentration. Figure 5SM shows the variations in substrate concentration as tyrosinase acts on the monophenol, assuming that the product, dopachrome, is stable. Note that the kinetic test of suicide substrates is fulfilled: the product accumulated at the end of the reaction, $[DC]_{\infty}$, is constant and the apparent inactivation constant $\lambda_{E_{ox}}^M$ varies hyperbolically with the concentration of monophenol, Fig. 5SM Inset, Eqns. (15–17).

Table 1. Confirmation by computer simulation and experimentation of the relations described in Eqn. (7) and Eqn. (10)

Results	Substrate	$[E]_0$ (mM)	$[NADH]_{ss}$ (μ M)	$[O_2]_{ss}$ (μ M)	$[DC]_{ss}$ (μ M)	r_D^{NADH}	r_D^{DC}	$r_{(MO)}^{O_2}$	$r_{(MO)}^{DC}$	Eqn. (7)	Eqn. (10)	$\lambda_{E_i}^D \times 10^3$ (min^{-1})	$\lambda_{E_i}^M \times 10^3$ (min^{-1})
Simulated							53500		53500	-	1		
	$[M]_0$ (1 mM)	0.10	-	-	10.70	-	-	-	-	-	-	-	8.1 ± 0.06
	$[D]_{ss}$ (46 μ M)	0.10	-	-	5.35	-	-	-	-	-	-	15.48 ± 0.06	-
	$[D]_0$ (1 mM)	0.10	-	-	5.35	-	-	-	-	-	-	73.26 ± 0.06	-
Experimental													
	$[M]_0$ (1 mM)	0.50	-	66.8 ± 0.1	-	-	-	-	43975 ± 2938	1.05	-	-	5.76 ± 0.06
	$[D]_{ss}$ (46 μ M)	0.50	$43.7 \pm 2.1^*$	-	-	-	-	-	-	-	-	$10.86 \pm 0.66^{**}$	-
	$[D]_0$ (1 mM)	0.50	44.9 ± 3.3	-	-	-	-	-	-	-	-	69.48 ± 6.12	-

$[D]_{ss} = 46 \mu\text{M}$ is the concentration of *o*-diphenol accumulated in the steady-state, when tyrosinase acts on 1 mM L-tyrosine. *Calculated from the *o*-diphenol accumulated in the steady-state of monophenolase activity, according to Eqn. (4). **Calculated from the *o*-diphenol accumulated in the steady-state of monophenolase activity, according to Eqn. (12).

ii) Presence of reductant. Simulation of the tyrosinase suicide inactivation as it acts on monophenols in the presence of reductant is shown in Fig. 6ASM, curve (a). In the same figure, curve (b) shows the inactivation in the same conditions but in the absence of reductant. Note the higher apparent inactivation constant in Fig. 6ASM, curve (a), than in Fig. 6ASM, curve (b). However, the value of the product accumulated at the end of the reaction in Fig. 6ASM, curve (a), is not double that shown in Fig. 6ASM, curve (b), as was the case for the diphenolase activity (Fig. 3SM), because, in the presence of reductant, the system is not in the steady-state and the relation between the turnovers of the oxidase and hydroxylase cycles is not maintained because *o*-diphenol is accumulated in the medium. The increased apparent inactivation constant can be explained by the result shown in Fig. 6BSM. Note that in Fig. 6BSM, curve (a), much more *o*-diphenol has been accumulated than in Fig. 6BSM, curve (b), so that the enzyme makes *r* turnovers (a fixed number) in the oxidase cycle more rapidly (in the presence of reductant). This acceleration of the inactivation is demonstrated in Fig. 6ASM, curve (a) and Fig. 6CSM, curve (a), which point to the accumulation of inactive enzyme with time. In Fig. 6CSM, curve (b), which represents the absence of reductant, the inactive enzyme, E_i , is accumulated in the medium with a smaller $\lambda_{E_i}^M$ than in the presence of reductant, Fig. 6CSM, curve (a).

The results obtained by simulation, Fig. 1SM–Fig. 6SM, from the mechanism proposed in Scheme I with $[M]_0=0$ and Scheme I and the value of 1 taken by Eqn. (10) (see Table 1), reveal that if this test could be demonstrated experimentally, it would be sufficient to confirm our hypothesis that tyrosinase acting on monophenols is not inactivated in the hydroxylase cycle but only in the oxidase cycle. This cycle arises from the accumulation of *o*-diphenol from the *o*-quinones and also through its enzymatic release from (*met*-tyrosinase-D)₃, Scheme I (Rodríguez-Lopez *et al.*, 1992a), and is responsible for the enzyme's inactivation as it acts in the oxidase cycle.

Experimental approach. Following the suicide inactivation kinetics of tyrosinase in its action on *o*-diphenols spectrophotometrically measuring NADH disappearance and in its reaction on monophenols by measuring oxygen consumption. The experimental approach involved checking that Eqn. (7) was fulfilled by spectrophotometrically measuring the suicide inactivation kinetics with *o*-diphenols (disappearance of NADH) and measuring the suicide inactivation of the monophenolase activity according to the oxygen consumed during the enzyme's action on monophenols.

The suicide inactivation of tyrosinase acting on L-dopa in the presence of NADH is described in (Munoz-Munoz *et al.*, 2010a). When the action of tyrosinase on L-tyrosine is studied at $t=0$ in the absence of *o*-diphenol, tyrosinase shows the typical lag period both in oxymetric and spectrophotometric assays: Fig. 1, curve (a) and Fig. 1 Inset, curve (a). The addition of *o*-diphenol brings the system to the steady-state at $t=0$, Fig. 1, curve (b) and Fig. 1 Inset, curve (b). In Fig. 1, curve (c) and in Fig. 1 Inset, curve (c), it can be seen that when NADH is added to the reaction medium along with *o*-diphenol, the latter continues to accumulate. The velocity continues to increase constantly and the system never reaches the steady-state, meaning that these suicide inactivation experiments involving monophenolase activity should never be carried out in the presence of NADH.

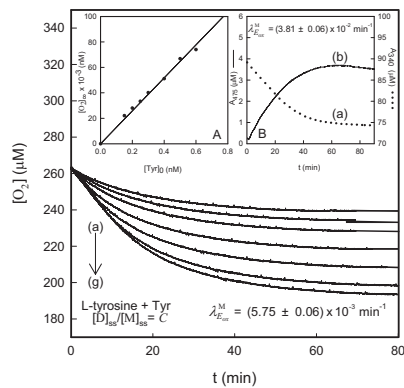


Figure 2. Indirect inactivation of tyrosinase in its action on L-tyrosine.

Oxymetric recordings of oxygen consumed in action of tyrosinase on L-tyrosine. The experimental conditions were 30 mM sodium phosphate buffer (pH 6.0), 25 °C, $[O_2]_0=0.26$ mM, $[L\text{-tyrosine}]_0=1$ mM, $[L\text{-dopa}]_0=46$ µM and the enzyme concentrations were (nM): (a) 0.15, (b) 0.20, (c) 0.25, (d) 0.30, (e) 0.40, (f) 0.50 and (g) 0.60. **Inset A.** Representation of the $[O_2]_{\infty}$ -values vs. initial enzyme concentration. **Inset B.** Curve (a), disappearance of NADH (0.095 mM) in action of tyrosinase (0.1 nM) on L-tyrosine (1 mM). The experimental conditions were the same as in Fig. 2. Curve (b), accumulation of dopachrome in the action of Tyr (1.5 nM) on L-tyrosine (1 mM).

Figure 2 shows the recordings of oxygen consumption as tyrosinase acts on L-tyrosine at different enzyme concentrations. Figure 2 Inset A shows the representation of the $[O_2]_{\infty}$ values vs. $[E]_0$ in the case of the suicide inactivation of tyrosinase in the monophenolase activity observed by measuring the disappearance of O_2 . Figure 2 Inset B, curve (a), depicts the inactivation of tyrosinase acting on L-tyrosine in the presence of NADH, while Fig. 2 Inset B, curve (b), depicts the inactivation observed by following dopachrome. Given the instability of dopachrome (data not shown) it is clear that its

measurement, Fig. 2 Inset B, curve (b), cannot be used since it evolves towards 5,6-dihydroxyindol (DHI) and 5,6-dihydroxyindolcarboxylic acid (DICA) (Riley, 1997). Non-linear regression analysis of the results shown here, Fig. 2 and Fig. 2 Inset B, curve (a), enables us to obtain the value of $\lambda_{E_{ox}}^M$, $[O_2]_{\infty}$ and $[NADH]_{\infty}$. Note the difference between the values of $\lambda_{E_{ox}}^M$ (Fig. 2 and Fig. 2 Inset B), a result that agrees with the numerical integrations shown in Fig. 6ASM and Fig. 6CSM.

These findings support and even confirm our hypothesis that the enzyme is not inactivated in the hydroxylase cycle. The experimental recordings shown in Fig. 2 give the values of $\lambda_{E_{ox}}^M$ and $[O_2]_{\infty}$. These data, together with the values of $[NADH]_{\infty}=[Q]_{\infty}$ obtained spectrophotometrically in the inactivation experiments with L-dopa (Munoz-Munoz *et al.*, 2010a), confirm the closeness to the value 1 as predicted by Eqn. (7) (see Table 2). The data also confirm that the monophenol delays the process of suicide inactivation, as we hypothesized. Hence, from Table 1, both in the experimental and simulated results $\lambda_{E_{ox}}^D/\lambda_{E_{ox}}^M \cong 12$ and 9, respectively, for the same concentration of substrate. These results agree with Eqns. (12) and (14) for *o*-diphenols and Eqns. (16) and (17) for monophenols.

Comparison of our model with that proposed by other authors

Other authors (Land *et al.*, 2007) have proposed an alternative model to explain suicide inactivation (Scheme IV). This mechanism describes the binding of the enzyme to a diphenol as if it were a monophenol, while the suicide inactivation occurs through the hydroxylase activity. The model implies:

- The structure of the substrate may influence whether suicide inactivation takes place,

Table 2. Kinetic constants which characterize the inactivation of E_d , E_m and E_d^* by dopa isomers and their protection by isomers of tyrosine under anaerobic conditions

Enzymatic form	Substrate	$K_E^{D(a)}$ (µM)	$k_{ID} \times 10^3$ (min ⁻¹)	$k_{ID}^* \times 10^3$ (min ⁻¹)	$K_E^{M(a)}$ (µM)
E_d^*	L-dopa	19.24 ± 2.12	–	0.25 ± 0.01	–
	D-dopa	28.88 ± 2.93	–	0.26 ± 0.02	–
	L-tyrosine	–	–	–	22.32 ± 3.96
	D-tyrosine	–	–	–	28.04 ± 4.85
E_d	L-dopa	10.77 ± 1.12	0.37 ± 0.01	–	–
	D-dopa	25.34 ± 2.24	0.37 ± 0.03	–	–
	L-tyrosine	–	–	–	23.95 ± 2.99
	D-tyrosine	–	–	–	29.02 ± 3.11
E_m	L-dopa	10.77 ± 1.12	0.37 ± 0.01	–	–
	D-dopa	25.34 ± 2.24	0.37 ± 0.03	–	–
	L-tyrosine	–	–	–	23.15 ± 2.51
	D-tyrosine	–	–	–	29.92 ± 3.16

^(a)In K_E^D and K_E^M , E corresponds to the enzymatic forms E_d^* or E_d . When the reaction is started with E_m , the data obtained correspond to E_d , because of the rapid transformation of E_m into E_d (Scheme VI).

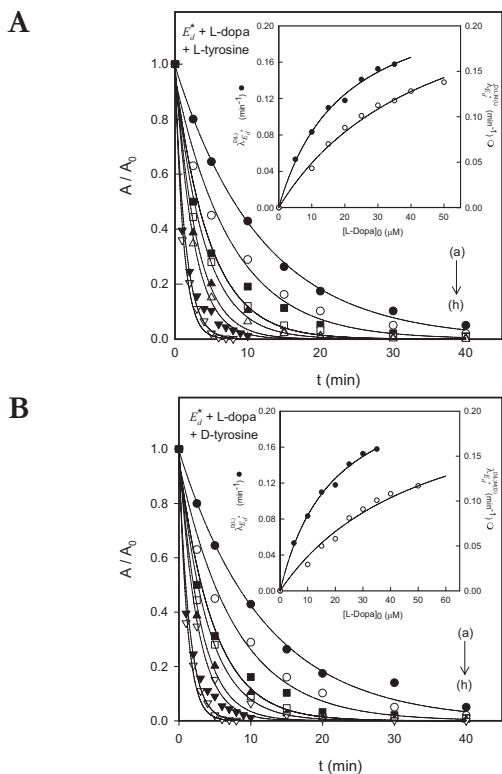


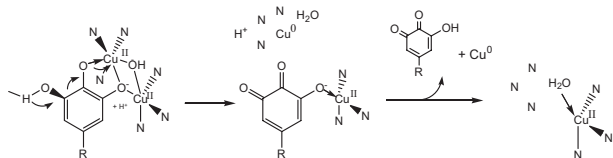
Figure 3. Effect of L-tyrosine and D-tyrosine on inactivation of E_d^* by L-dopa.

The inactivation of E_d^* by L-dopa was studied after generating it as described in Material and methods. **(A)** Effect of L-tyrosine. The o-diphenol and the monophenol (L-tyrosine) was added at $t=0$ and aliquots were taken at different times to measure the residual activity with 2.5 mM L-dopa ($\lambda=475$ nm). The experimental conditions were: 30 mM sodium phosphate buffer (pH 6.0), 25°C, $[E]_0=0.1$ μ M (see Material and Methods section), $[H_2O_2]_0=2$ μ M and $[L\text{-tyrosine}]_0=20$ μ M. The L-dopa concentrations were (μ M): (a) 10 \bullet , (b) 15 \circ , (c) 20 \blacksquare , (d) 25 \square , (e) 30 \blacktriangle , (f) 35 \triangle , (g) 40 \blacktriangledown and (h) 50 \triangledown . The experimental results were fitted to Eqn. (18) and the apparent inactivation constants to Eqn. (19). **Inset.** Representation of the values of $\lambda_{E_d^*}^{D(L)M(L)}$ vs. $[L\text{-dopa}]_0$ in the presence (O) of L-tyrosine and of $\lambda_{E_d^*}^{D(L)}$ vs. $[L\text{-dopa}]_0$ in its absence (\bullet). **(B)** Effect of D-tyrosine. The experimental conditions were the same as in (A) but with 40 μ M D-tyrosine. The experimental results were fitted to Eqn. (18) and the apparent inactivation constants to Eqn. (19). The L-dopa concentrations were (μ M): (a) 10 \bullet , (b) 15 \circ , (c) 20 \blacksquare , (d) 25 \square , (e) 30 \blacktriangle , (f) 35 \triangle , (g) 40 \blacktriangledown and (h) 50 \triangledown . **Inset.** Representation of the values of $\lambda_{E_d^*}^{D(L)M(D)}$ vs. $[L\text{-dopa}]_0$ in the presence (O) of D-tyrosine and of $\lambda_{E_d^*}^{D(L)}$ vs. $[L\text{-dopa}]_0$ in its absence (\bullet).

- The enzymes catechol oxidase should not suffer inactivation since they have no hydroxylase activity.

Let us look at these two implications below:

i) Scheme IV (Land *et al.*, 2007; 2008; Ramsden *et al.*, 2009) implies that the chemical structure of the substrate is of fundamental importance for suicide inactivation: the substrate must have at least two hydroxyl groups in *ortho* in the benzene ring. Hence, when the



Scheme IV. Proposed model to explain the suicide inactivation of tyrosinase during its monophenolase activity when it acts on o-diphenols (Land *et al.*, 2007).

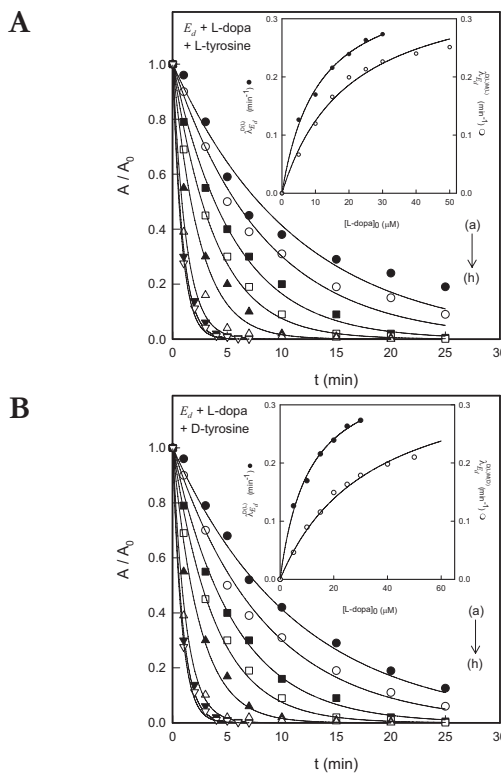


Figure 4. Effect of L-tyrosine and D-tyrosine on inactivation of E_d by L-dopa.

(A) Effect of L-tyrosine. The form E_d was obtained as described in Material and methods and immediately incubated with o-diphenol and monophenol (L-tyrosine), taking aliquots at different times to measure the residual activity with 2.5 mM L-dopa ($\lambda=475$ nm). The experimental conditions were: 30 mM sodium phosphate buffer (pH 6.0), 25°C, $[E]_0=0.1$ μ M (see Material and Methods section), $[H_2O_2]_0=2$ μ M and $[L\text{-tyrosine}]_0=20$ μ M. The L-dopa concentrations were (μ M): (a) 5 \bullet , (b) 10 \circ , (c) 15 \blacksquare , (d) 20 \square , (e) 25 \blacktriangle , (f) 30 \triangle , (g) 40 \blacktriangledown and (h) 50 \triangledown . The experimental results were fitted to Eq. (21) and the apparent inactivation constants to Eqn. (22). **Inset.** Representation of the values of $\lambda_{E_d}^{D(L)M(L)}$ vs. $[L\text{-dopa}]_0$ in the presence (O) of L-tyrosine and of $\lambda_{E_d}^{D(L)}$ vs. $[L\text{-dopa}]_0$ in its absence (\bullet). **(B)** Effect of D-tyrosine. The experimental conditions were the same as in (A) but with 40 μ M D-tyrosine. The L-dopa concentrations were (μ M): (a) 5 \bullet , (b) 10 \circ , (c) 15 \blacksquare , (d) 20 \square , (e) 25 \blacktriangle , (f) 30 \triangle , (g) 40 \blacktriangledown and (h) 50 \triangledown . The experimental results were fitted to Eqn. (21) and the apparent inactivation constants to Eqn. (22). **Inset.** Representation of the values of $\lambda_{E_d}^{D(L)M(D)}$ vs. $[L\text{-dopa}]_0$ in the presence (O) of D-tyrosine and of $\lambda_{E_d}^{D(L)}$ vs. $[L\text{-dopa}]_0$ in its absence (\bullet). In the case of E_{mr} , the results are the same as those for E_d (see Table 2).

substrate is a trihydroxybenzene (e.g., pyrogallol), the proposed mechanism (Scheme IV) would indicate that this compound is not a suicide substrate (Land *et al.*, 2007), although our experimental results (Munoz-Munoz *et al.*, 2008) suggest that it is the most powerful suicide substrate of mushroom tyrosinase. The oxygen consumption that is observed is due to autooxidation (Munoz-Munoz *et al.*, 2008), not to the action of the enzyme. Indeed, the addition of superoxide dismutase and catalase to the medium inhibits this autooxidation process, underlining that pyrogallol is really a suicide substrate.

ii) The enzymes catechol oxidase should not suffer inactivation since they have no hydroxylase activity. The catechol oxidases studied to date in this respect are those of *Ipomoea batatas*, *Lycopus europaeus*, *Populus nigra* and *Aspergillus oryzae* (Klabunde *et al.*, 1998; Rompel *et al.*, 1999; Gasparetti *et al.*, 2010). The reason for choosing these oxidases is that these enzymes

have no monophenolase activity and so suicide inactivation will not occur. The authors (Land *et al.*, 2007; 2008; Ramsden *et al.*, 2009) chose banana enzyme (*Musa cavendishii*), but the experiments depicted in Fig. 1 of Land *et al.* (2008) are carried out at such a short time scale and with such a high concentration of the enzyme that practically all the oxygen is consumed. Moreover, this enzyme possesses monophenolase activity (Padron *et al.*, 1974) and suicide activation has been described when it acts on catechol (Padron *et al.*, 1975). However, in (Land *et al.*, 2008), differences in the mass spectra are seen depending on whether the experiments are carried out with mushroom or banana tyrosinase (Land *et al.*, 2008). The polyphenol oxidases studied to date – apple, pear, avocado and strawberry (Espin *et al.*, 1995; 1997a; 1997b; 1997c; 1997d) – show two activities, monophenolase and diphenolase, the first rather low. In short, the tests should have been carried out at long measuring times and with low enzyme concentrations.

The experimental results of the test proposed in the present study in relation to the model of Scheme I, see Table 1, give weight to the mechanism that we propose that only during the diphenolase activity of tyrosinase is the enzyme inactivated.

Effect of monophenols on tyrosinase under anaerobic conditions

Effect of monophenols on E_d , E_d^* and E_m . When each of these enzymatic forms was generated anaerobically and preincubated with L-tyrosine or D-tyrosine, no inactivation was observed (result not shown). Under anaerobic conditions, therefore, tyrosinase is not inactivated by monophenols.

Effect of L-tyrosine and D-tyrosine on inactivation of E_d , E_d^* and E_m by *o*-diphenols. When the experiments of inactivation by diphenols (Munoz-Munoz *et al.*, 2010a) were carried out in the presence of L-tyrosine, the results (Fig. 3A) showed that inactivation is delayed according to the mechanism depicted in Scheme VA.

The experimental results (Fig. 3A) were fitted to Eqn. (18).

$$[E_d^*] = [E_d^*]_0 e^{-\lambda_{E_d^*}^{D(L)M(L)} t} \quad (18)$$

The values of $\lambda_{E_d^*}^{D(L)M(L)}$ (Fig. 3A Inset) were fitted to Eqn. (19):

$$\lambda_{E_d^*}^{D(L)M(L \text{ or } D)} = \frac{k_{iD(L)M(L \text{ or } D)}^* [D]_0}{K_{E_d^*}^{D(L)M(L \text{ or } D)} + [D]_0} \quad (19)$$

where $\lambda_{E_d^*}^{D(L)M(L)}$ is the apparent inactivation constant of E_d^* for L-dopa in the presence of L-tyrosine. Note how $k_{iD(L)M(L)}$ takes the same value as $k_{iD(L)}$ (Munoz-Munoz *et al.*, 2010a), although $K_{E_d^*}^{D(L)}$ is greater than $K_{E_d^*}^{D(L)}$, according to Eqn. (20):

$$K_{E_d^*}^{D(L)M(L \text{ or } D)} = K_{E_d^*}^{D(L)} \left(1 + \frac{[M]_0}{K_{E_d^*}^{M(L \text{ or } D)}} \right) \quad (20)$$

where $K_{E_d^*}^{M(L)}$ is the dissociation constant of the complex E_d^*M (Table 2). When D-tyrosine is used (Fig. 3B), the experimental data can be fitted to Eqn. (18) and subsequently the values of $\lambda_{E_d^*}^{D(L)M(L)}$ (Fig. 3B Inset) to Eqn. (19), obtaining $k_{iD(L)M(D)}^*$ and $K_{E_d^*}^{D(L)M(D)}$. Note how $k_{iD(L)M(D)}^*$ takes on the same value as $k_{iD(L)}$ (Munoz-Munoz *et*

al., 2010a), although $K_{E_d^*}^{D(L)M(D)}$ is greater than $K_{E_d^*}^{D(L)}$. From Eqn. (20), one obtains the $K_{E_d^*}^{D(L)M(D)}$ (Table 2), the value of which is only slightly greater than $K_{E_d^*}^{D(L)}$, the E_d^* form of the enzyme showing stereospecificity for the binding of the isomers L- and D-tyrosine. As occurred with L- and D-dopa, although the values of δ_4 for L- and D-tyrosine are the same ($\delta_4=158.86$ p.p.m.), stereospecific effects are originated in the binding. This effect is less pronounced than in the case of *o*-diphenols because the latter bind to two atoms of copper (Table 2).

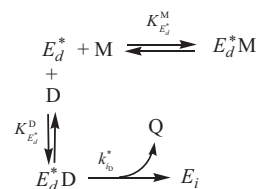
The same experiments carried out with the E_d and E_m forms (Fig. 4A and Fig. 4B) can be fitted to Eqns. (21), (22) and (23) (Scheme VB and VI).

$$[E_d] = [E_d]_0 e^{-\lambda_{E_d}^{D(L)M(L)} t} \quad (21)$$

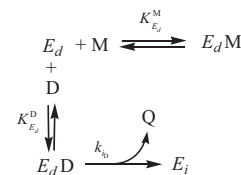
$$\lambda_{E_d}^{D(L)M(L \text{ or } D)} = \frac{k_{iD(L)M(L \text{ or } D)} [D]_0}{K_{E_d}^{D(L)M(L \text{ or } D)} + [D]_0} \quad (22)$$

and

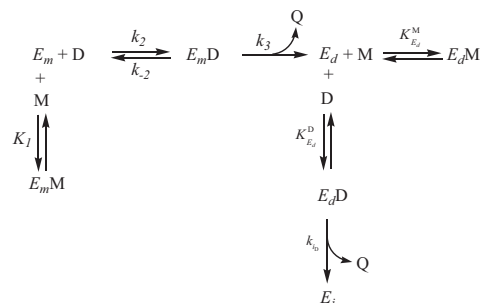
$$K_{E_d}^{D(L)M(L \text{ or } D)} = K_{E_d}^{D(L)} \left(1 + \frac{[M]_0}{K_{E_d}^{M(L \text{ or } D)}} \right) \quad (23)$$



Scheme VA. Effect of monophenols on E_d^* , inactivation by *o*-diphenol.



Scheme VB. Effect of monophenols on E_d , inactivation by *o*-diphenol.



Scheme VI. Effect of monophenols on E_m , inactivation by *o*-diphenol.

Analysis of the data (Fig. 4A Inset and Fig. 4B Inset) provides the values of $k_{iD(L)M(L)}$ and $k_{iD(L)M(D)}$ which are the same as $k_{iD(L)}$ (Munoz-Munoz *et al.*, 2010a), although, once again, the values of $K_{E_d}^{D(L)M(D)}$ are greater than those

of $K_{Ed}^{D(L)}$, Eqn. (23) (Table 2). From the same equation $K_{Ed}^{M(L)}$ and $K_{Ed}^{M(D)}$ can be obtained for the binding of L-tyrosine and D-tyrosine to the form E_d and, once again, a stereospecific binding pattern can be observed, which is better for L than for D (Table 2). Since E_m is rapidly transformed into E_d (Scheme VI), any information gained in a kinetic study of the form E_m is the same as for the E_d (Table 2).

CONCLUSIONS

Monophenols protect the enzyme from inactivation by *o*-diphenols. However, under aerobic conditions, due to the accumulation of *o*-diphenol in the medium through the chemical evolution of the *o*-dopaquinone and its enzymatic release, the enzyme is inactivated. Therefore, it might be said that the monophenols inactivate the enzyme through an indirect process.

Acknowledgements

This paper was partially supported by grants from the Ministerio de Educación y Ciencia (Madrid, Spain) Project BIO2009-12956, from the Fundación Séneca (CARM, Murcia, Spain) Projects 08856/PI/08 and 08595/PI/08, from the Consejería de Educación (CARM, Murcia, Spain) BIO-BMC 06/01-0004 and from FISCAM PI-2007/53 from the Consejería de Salud y Bienestar Social de la Junta de Comunidades de Castilla La Mancha. F.G.M. and J.L.M.M. have two fellowships from Fundación Caja Murcia (Murcia, Spain).

REFERENCES

- Aasa R, Deinum J, Lerch K, Reinhammar B (1978) The reaction of mercaptans with tyrosinases and hemocyanins. *Biochim Biophys Acta* **535**: 287–298.
- Asimov I, Dawson CR (1950) On the reaction inactivation of tyrosinase during the aerobic oxidation of catechol. *J Am Chem Soc* **72**: 820–828.
- Battaini G, Monzani E, Casella L, Lonardi L, Tepper AW, Canters GW, Bubacco L (2002) Tyrosinase-catalyzed oxidation of fluorophenols. *J Biol Chem* **277**: 44606–44612.
- Beltramini M, Lerch K (1982) Fluorescence properties of Neurospora tyrosinase. *Biochem J* **205**: 173–180.
- Cabanes J, Garcia-Canovas F, Lozano JA, Garcia-Carmona F (1987) A kinetic study of the melanization pathway between L-tyrosine and dopachrome. *Biochim Biophys Acta* **923**: 187–195.
- Casella L, Monzani E, Gulloti M, Cavagnino D, Cerina G, Santagostini L, Ugo R (1996) Functional modeling of tyrosinase. Mechanism of phenol ortho-hydroxylation by dinuclear copper complexes. *Inorg Chem* **35**: 7516–7525.
- Chang TS (2007) Two potent suicide substrates of mushroom tyrosinase: 7,8,4'-trihydroxyisoflavone and 5,7,8,4'-tetrahydroxyisoflavone. *J Agric Food Chem* **55**: 2010–2015.
- Chang TS (2009) An updated review of tyrosinase inhibitors. *Int J Mol Sci* **16**: 2440–2475.
- Chang TS, Lin MY, Lin HJ (2010) Identifying 8-hydroxynaringenin as a suicide substrate of mushroom tyrosinase. *J Cosmet Sci* **61**: 205–210.
- Chazarra S, Cabanes J, Escribano J, Garcia-Carmona F (1997) Kinetic study of the suicide inactivation of latent polyphenoloxidase from iceberg lettuce (*Lactuca sativa*) induced by 4-tert-butylcatechol in the presence of SDS. *Biochim Biophys Acta* **1339**: 297–303.
- Decker H, Schweikardt T, Tuzcek F (2006) The first crystal structure of tyrosinase: All questions answered?. *Angew Chem Int Ed* **45**: 4546–4550.
- Deinum J, Lerch K, Reinhammar B (1976) An EPR study of Neurospora tyrosinase. *FEBS Lett* **69**: 161–164.
- Dieter C, Lerch K (1982) In *Oxidases and Related Redox Systems*. King TE, Mason HS, Morrison M, eds, pp 305–317. Pergamon Press, New York.
- Espin JC, Morales M, Varon R, Tudela J, Garcia-Canovas F (1995) Monophenolase activity of polyphenol oxidase from verdedoncella apple. *J Agric Food Chem* **43**: 2807–2812.
- Espin JC, Morales M, Varon R, Tudela J, Garcia-Canovas F (1997a) Monophenolase activity of polyphenol oxidase from Blanquilla pear. *Phytochemistry* **44**: 17–22.
- Espin JC, Ochoa M, Tudela J, Garcia-Canovas F (1997b) Monophenolase activity of strawberry polyphenol oxidase. *Phytochemistry* **45**: 667–670.
- Espin JC, Tudela J, Garcia-Canovas F (1997c) Monophenolase activity of polyphenol oxidase from artichoke heads (*Cynara scolymus* L.). *Food Science Technology-Lebensmittel-Wissenschaft Technologie* **30**: 819–825.
- Espin JC, Trujano MF, Tudela J, Garcia-Canovas F (1997d) Monophenolase activity of polyphenol oxidase from Haas avocado. *J Agric Food Chem* **45**: 1091–1096.
- Penoll L, Peñalver MJ, Rodriguez-Lopez JN, Garcia-Ruiz PA, Garcia-Canovas F, Tudela J (2004) Deuterium isotope effect on the oxidation of monophenols and *o*-diphenols by tyrosinase. *Biochem J* **380**: 643–650.
- Garcia-Canovas F, Garcia-Carmona F, Vera-Sanchez J, Iborra-Pastor JL, Lozano-Teruel JA (1982) The role of pH in the melanin biosynthesis pathway. *J Biol Chem* **257**: 8738–8744.
- Garcia-Canovas F, Tudela J, Martinez-Madrid C, Varon R, Garcia-Carmona F, Lozano JA (1987) Kinetic study on the suicide inactivation of tyrosinase induced by catechol. *Biochim Biophys Acta* **912**: 417–423.
- Garcia-Carmona F, Garcia-Canovas F, Iborra JL, Lozano JA (1982) Kinetic study of the pathway of melanization between L-dopa and dopachrome. *Biochim Biophys Acta* **717**: 124–131.
- Garcia-Molina F, Muñoz JL, Varon R, Rodriguez-Lopez JN, Garcia-Canovas F, Tudela J (2007) A review on spectrophotometric methods for measuring the monophenolase and diphenolase activities of tyrosinase. *J Agric Food Chem* **55**: 9739–9749.
- Garcia-Sevilla F, Garrido del Solo C, Duggleby RG, Garcia-Canovas F, Peyro R, Varon R (2000) Use of a window program for simulation of the progress curves of reactants and intermediates involved in enzyme-catalyzed reactions. *Biosystems* **54**: 151–164.
- Gasparrini C, Faccio G, Arvas M, Buchert J, Saloheimo M, Kruus K (2010) Discovery of a new tyrosinase-like enzyme family lacking a C-terminally processed domain: production and characterization of an *Aspergillus oryzae* catechol oxidase. *App Microbiol Biotechnol* **86**: 213–226.
- Ingraham LL, Corse J, Makower B (1952) Enzymatic browning of fruits. 3. Kinetics of the reaction inactivation of polyphenol oxidase. *J Am Chem Soc* **74**: 2623–2626.
- Ismaya WT, Rozeboom HJ, Schurink M, Boeriu CG, Wichers H, Dijkstra BW (2011) Crystallization and preliminary X-ray crystallographic analysis of tyrosinase from the mushroom *Agaricus bisporus*. *Acta Crystallogr Sect F, Struct Biol Cryst Commun* **67**: 575–578.
- Itoh S, Fukuzumi S (2007) Monooxygenase activity of type 3 copper proteins. *Acc Chem Res* **40**: 592–600.
- Jackman M, Huber M, Hajnal A, Lerch K (1992) Stabilization of the oxy form of tyrosinase by a single conservative amino acid substitution. *Biochem J* **282**: 915–918.
- Jandel scientific. *Sigma Plot 9.0 for Windows™*; Jandel scientific: Core Madera 2006.
- Jolley Jr RL, Evans LH, Makino N, Mason HS (1974) Oxytyrosinase. *J Biol Chem* **249**: 335–345.
- Karlin KD, Lee D-H, Obias HV, Humphreys KF (1998) Copper-dioxygen complexes: Functional models for proteins. *Pure Appl Chem* **70**: 855–862.
- Klabunde T, Eicken C, Sachetti JC, Krebs B (1998) Crystal structure of a plant catechol oxidase containing a dicopper center. *Nat Struct Biol* **5**: 1084–1090.
- Land EJ, Ramsden CA, Riley PA (2007) The mechanism of suicide-inactivation of tyrosinase: A substrate structure investigation. *Toboku J Exp Med* **212**: 341–348.
- Land EJ, Ramsden CA, Riley PA, Stratford MR (2008) Evidence consistent with the requirement of cresolase activity for suicide inactivation of tyrosinase. *Toboku J Exp Med* **216**: 231–238.
- Lerch K (1983) Neurospora tyrosinase: structural, spectroscopic and catalytic properties. *Mol Cell Biochem* **52**: 125–138.
- Lowry OH, Rosebrough NJ, Farr AL, Randall RJ (1951) Protein measurement with the Folin phenol reagent. *J Biol Chem* **193**: 265–275.
- Marino SM, Fogal S, Bisaglia M, Moro S, Scartabelli G, De Gioia L, Spada A, Monzani E, Casella L, Mammì S, Bubacco L (2011) Investigation of *Streptomyces antibioticus* tyrosinase reactivity towards chlorophenols. *Arch Biochem Biophys* **505**: 67–74.
- Matoba Y, Kumagai T, Yamamoto A, Yoshitsu H, Sugiyama M (2006) Crystallographic evidence that the dinuclear copper center of tyrosinase is flexible Turing catalysis. *J Biol Chem* **281**: 8981–8990.
- Miller SM, Klinman JP (1985) Secondary isotope effects and structure-reactivity correlations in the dopamine β -monooxygenase reaction: Evidence for a chemical mechanism. *Biochemistry* **24**: 2114–2127.
- Molina FG, Muñoz JL, Varon R, Rodriguez Lopez JN, Garcia-Canovas F, Tudela J (2007) An approximate analytical solution to the lag period of the monophenolase activity of tyrosinase. *Int J Biochem Cell Biol* **39**: 238–252.
- Monzani E, Quinti L, Perotti A, Casella L, Gulloti M, Randaccio L, Geremia S, Nardin G, Faleschini P, Tabbi G (1998) Tyrosinase

- models. Synthesis, structure, catechol oxidase activity, and phenol monoxygenase activity of a dinuclear copper complex derived from a triamino pentabenzimidazole ligand. *Inorg Chem* **37**: 553–562.
- Muñoz-Muñoz JL, García-Molina F, García-Ruiz PA, Molina-Alarcon M, Tudela J, García-Canovas F, Rodríguez-Lopez JN (2008) Phenolic substrates and suicide inactivation of tyrosinase: kinetics and mechanism. *Biochem J* **416**: 413–440.
- Muñoz-Muñoz JL, García-Molina F, García-Ruiz PA, Varon R, Tudela J, García-Canovas F, Rodríguez-Lopez JN (2009) Stereospecific inactivation of tyrosinase by L- and D-ascorbic acid. *Biochim Biophys Acta* **1794**: 244–253.
- Muñoz-Muñoz JL, Acosta-Motos JR, García-Molina F, Varon R, García-Ruiz PA, Tudela J, García-Canovas F, Rodríguez-Lopez JN (2010a) Tyrosinase inactivation in its action on L-dopa. *Biochim Biophys Acta* **1804**: 1467–1475.
- Muñoz-Muñoz JL, García-Molina F, Varon R, García-Ruiz PA, Tudela J, García-Canovas F, Rodríguez-Lopez JN (2010b) Suicide inactivation of the diphenolase and monophenolase activities of tyrosinase. *IUBMB Life* **62**: 539–547.
- Muñoz-Muñoz JL, García-Molina F, García-Ruiz PA, Varon R, Tudela J, García-Canovas F, Rodríguez-Lopez JN (2010c) Some kinetic properties of deoxytyrosinase. *J Mol Cat B: Enzymatic* **62**: 173–182.
- Nelson JM, Dawson CR (1944) Tyrosinase. *Adv Enzymol* **4**: 99–152.
- Padron MP, Gonzalez AG, Lozano JA (1974) O-diphenol:oxygen-oxidoreductase from *Musa cavendishii*. *Rev Esp Fisiol* **30**: 167–176.
- Padron MP, Lozano JA, Gonzalez AG (1975) Properties of o-diphenol:O₂ oxidoreductase from *Musa cavendishii*. *Phytochemistry* **14**: 1959–1963.
- Peñalver MA, Rodríguez-Lopez JN, García-Ruiz PA, García-Canovas F, Tudela J (2003) Solvent deuterium isotope effect on the oxidation of o-diphenols by tyrosinase. *Biochim Biophys Acta* **1650**: 128–135.
- Ramsden CA, Stratford MRL, Riley PA (2009) The influence of catechol structure on the suicide-inactivation of tyrosinase. *Org Biomol Chem* **7**: 3388–3390.
- Riley PA (1997) Melanin. *Int J Biochem Cell Biol* **29**: 1235–1239.
- Ramsden CA, Riley PA (2010a) Mechanistic studies of tyrosinase suicide inactivation. *ARKIVOC* (i): 260–274.
- Ramsden CA, Riley PA (2010b) Studies of the competing rates of catechol oxidation and suicide inactivation of tyrosinase. *ARKIVOC* (x): 248–254.
- Rodríguez-Lopez JN, Tudela J, Varon R, García-Carmona F, García-Canovas F (1992a) Analysis of a kinetic model for melanin biosynthesis pathway. *J Biol Chem* **267**: 3801–3810.
- Rodríguez-Lopez JN, Ros-Martínez JR, Varon R, García-Canovas F (1992b) Calibration of a Clark-type oxygen electrode by tyrosinase catalyzed-oxidation of 4-tert-butylcatechol. *Anal Biochem* **202**: 356–360.
- Rodríguez-Lopez JN, Fenoll LG, García-Ruiz PA, Varon R, Tudela J, Thorneley RN, García-Canovas F (2000) Stopped-flow and steady-state study of the diphenolase activity of mushroom tyrosinase. *Biochemistry* **39**: 10497–10506.
- Rolff M, Schottenheim J, Decker H, Tuzcek F (2011) Copper-O₂ reactivity of tyrosinase models towards external monophenolic substrates: molecular mechanism and comparison with the enzyme. *Chem Soc Rev* **40**: 4077–4098.
- Rompel A, Fisher H, Meiwes D, Buldt-Karentzopoulos K, Dillinger R, Tuzcek F, Witzel H, Krebs B (1999) Purification and spectroscopic studies on catechol oxidase from *Lycopodium europaeus* and *Populus nigra*: Evidence for a dinuclear copper center of type and spectroscopic similarities to tyrosinase and hemocyanin. *J Biol Inorg Chem* **4**: 56–63.
- Ros JR, Rodríguez-Lopez JN, García-Canovas F (1994) Tyrosinase: kinetic analysis of the transient phase and the steady state. *Biochim Biophys Acta* **1204**: 33–42.
- Sanchez-Ferrer A, Rodríguez-Lopez JN, García-Canovas F, García-Carmona F (1995) Tyrosinase: a comprehensive review of its mechanism. *Biochim Biophys Acta* **1247**: 1–11.
- Seiji M, Sasaki M, Tomita Y (1978) Nature of tyrosinase inactivation in melanosomes. *Tohoku J Exp Med* **125**: 233–245.
- Sendovski M, Kanteev M, Shuster Ben-Yosef V, Adir N, Fishman A (2010) Crystallization and preliminary X-ray crystallographic analysis of a bacterial tyrosinase from *Bacillus megaterium*. *Acta Crystallogr Sect F, Struct Biol Cryst Commun* **66**: 1101–1103.
- Sendovski M, Kanteev M, Shuster Ben-Yosef V, Adir N, Fishman A (2011) First structures of an active bacterial tyrosinase reveal copper plasticity. *J Mol Biol* **405**: 227–237.
- Solomon EI, Sundaram UM, Machonkin TE (1996) Multicopper oxidases and oxygenases. *Chem Rev* **96**: 2563–2606.
- Tai SS-K, Lin C-G, Wu M-H, Chang TS (2009) Evaluation of depigmenting activity by 8-hydroxydaidzein in mouse B16 melanoma cells and human volunteers. *Int J Mol Sci* **10**: 4257–4266.
- Tomita Y, Seiji M (1977) Inactivation mechanism of tyrosinase in mouse melanoma. *J Dermatol* **4**: 245–249.
- Tomita Y, Hariu A, Mizuno C, Seiji M (1980) Inactivation of tyrosinase by dopa. *J Invest Dermatol* **75**: 379–382.
- Tudela J, García-Canovas F, Varon R, García-Carmona F, Galvez J, Lozano JA (1987) Transient-phase kinetics of enzyme inactivation induced by suicide substrates. *Biochim Biophys Acta* **912**: 408–416.
- Tyeklar Z, Karlin KD (1989) Copper-dioxygen complexes: A bioinorganic challenge. *Acc Chem Res* **22**: 241–248.
- Waley S (1980) Kinetics of suicide substrates. *Biochem J* **185**: 771–773.
- Waley SG (1985) Kinetics of suicide substrates. Practical procedures for determining parameters. *Biochem J* **227**: 843–849.